PNAS RESEARCH ARTICLE | PHYSIOLOGY OPEN ACCESS

Acute phosphatidylinositol 4,5 bisphosphate depletion destabilizes sarcolemmal expression of cardiac L-type Ca^{2+} channel $Ca_V1.2$

Taylor L. Voelker[a], Silvia G. del Villar[a], Maartje Westhoff[a], Alexandre D. Costa[a], Andrea M. Coleman[b], Johannes W. Hell[b], Mary C. Horne[b], Eamonn J. Dickson[a], and Rose E. Dixon[a,1]

Edited by Scott Earley, University of Nevada Reno, Reno, NV; received December 14, 2022; accepted March 3, 2023 by Editorial Board Member Mark T. Nelson

$Ca_V1.2$ channels are critical players in cardiac excitation–contraction coupling, yet we do not understand how they are affected by an important therapeutic target of heart failure drugs and regulator of blood pressure, angiotensin II. Signaling through G_q-coupled AT1 receptors, angiotensin II triggers a decrease in PIP_2, a phosphoinositide component of the plasma membrane (PM) and known regulator of many ion channels. PIP_2 depletion suppresses $Ca_V1.2$ currents in heterologous expression systems but the mechanism of this regulation and whether a similar phenomenon occurs in cardiomyocytes is unknown. Previous studies have shown that $Ca_V1.2$ currents are also suppressed by angiotensin II. We hypothesized that these two observations are linked and that PIP_2 stabilizes $Ca_V1.2$ expression at the PM and angiotensin II depresses cardiac excitability by stimulating PIP_2 depletion and destabilization of $Ca_V1.2$ expression. We tested this hypothesis and report that $Ca_V1.2$ channels in tsA201 cells are destabilized after AT1 receptor-triggered PIP_2 depletion, leading to their dynamin-dependent endocytosis. Likewise, in cardiomyocytes, angiotensin II decreased t-tubular $Ca_V1.2$ expression and cluster size by inducing their dynamic removal from the sarcolemma. These effects were abrogated by PIP_2 supplementation. Functional data revealed acute angiotensin II reduced $Ca_V1.2$ currents and Ca^{2+} transient amplitudes thus diminishing excitation–contraction coupling. Finally, mass spectrometry results indicated whole-heart levels of PIP_2 are decreased by acute angiotensin II treatment. Based on these observations, we propose a model wherein PIP_2 stabilizes $Ca_V1.2$ membrane lifetimes, and angiotensin II-induced PIP_2 depletion destabilizes sarcolemmal $Ca_V1.2$, triggering their removal, and the acute reduction of $Ca_V1.2$ currents and contractility.

L-type calcium channels | PIP_2 | EC-coupling | ion channel trafficking | angiotensin II

Voltage-gated L-type $Ca_V1.2$ Ca^{2+} channels are depolarization-triggered conduits of Ca^{2+} entry into excitable cells. In the heart, they are critical players in excitation-contraction (EC) coupling, where they provide the initial, predominantly t-tubule localized entry pathway for Ca^{2+} (1). During the peak and plateau phases of the ventricular action potential, $Ca_V1.2$-conducted Ca^{2+} influx activates a larger release of sarcoplasmic reticulum (SR) Ca^{2+} from clusters of type 2 ryanodine receptors (RyR2) on the juxtaposed junctional SR via Ca^{2+}-induced Ca^{2+}-release (CICR). The magnitude of local CICR and its summation across thousands of sites within each cardiomyocyte dictates the amplitude of the global Ca^{2+} transient and the strength of the subsequent myocardial contraction. As release of SR Ca^{2+} is graded by the amplitude of Ca^{2+} entry through $Ca_V1.2$ channels, alterations in the number and/or activity of $Ca_V1.2$ channels on the t-tubule sarcolemma tunes EC-coupling (2).

Physiological signaling cascades (3–6), post-translational modifications (7–11), and Ca^{2+} itself (12–16) are well-studied regulators of both $Ca_V1.2$ channel activity and sarcolemmal expression in various tissues, including the heart. However, even though $Ca_V1.2$ channels are embedded in a lipid environment, and despite the fact that many other ion channels and exchangers are known to be regulated by the membrane phospholipid phosphatidylinositol 4,5 bisphosphate ($PI(4,5)P_2$, henceforth abbreviated as PIP_2), its potential effects on $Ca_V1.2$ distribution, activity, and expression in cardiomyocytes have been overlooked. There is accumulating evidence that several subtypes of voltage-gated Ca^{2+} channels are regulated by PIP_2; however, the experiments underlying these findings have largely been carried out in heterologous expression systems (17–20), neurons (21), or pancreatic β-cells (22) and were not done in cardiomyocytes. These previous reports indicate that $Ca_V1.2$ currents are suppressed upon depletion of PIP_2 downstream of G_q-coupled activation of M_1-muscarinic receptors (M_1R) by oxotremorine-m (Oxo-m) or through

Significance

The potent vasopressor angiotensin II is released acutely during blood pressure control, and chronically during heart failure as a physiological strategy to increase cardiac output. We propose a mechanism, whereby angiotensin II signaling in ventricular myocytes stimulates hydrolysis of a membrane phospholipid called PIP_2, triggering $Ca_V1.2$ channel internalization, and providing a means to acutely tune cellular excitability and modulate cardiac excitation-contraction coupling. Accordingly, this study presents data that supports a novel mechanistic role of PIP_2 as a stabilizer of $Ca_V1.2$ channel expression on the sarcolemma of ventricular myocytes. Moreover, we provide the evidence that physiological signaling pathways alter cardiac PIP_2 levels, and thus this work has implications for the many cardiac ion channels and exchangers regulated by PIP_2.

Author contributions: J.W.H., M.C.H., E.J.D., and R.E.D. designed research; T.L.V., S.G.d.V., M.W., A.D.C., A.M.C., and E.J.D. performed research; T.L.V., S.G.d.V., M.W., A.D.C., A.M.C., and E.J.D. analyzed data; and T.L.V. and R.E.D. wrote the paper.

The authors declare no competing interest.

This article is a PNAS Direct Submission. S.E. is a guest editor invited by the Editorial Board.

[1]To whom correspondence may be addressed. Email: redickson@ucdavis.edu.

This article contains supporting information online at https://www.pnas.org/lookup/suppl/doi:10.1073/pnas.2221242120/-/DCSupplemental.

Published March 28, 2023.

activation of a voltage-sensitive 5-phosphatase DR-VSP that removes the 5′ phosphate from $PI(4,5)P_2$ and converts it to PI(4)P (17, 20). However, how PIP_2 regulates $Ca_V1.2$ remains unknown.

During G_q-coupled physiological signaling cascades, PIP_2 levels in the plasma membrane (PM) fall due to its phospholipase C (PLC)-mediated hydrolysis, generating inositol trisphosphate (IP_3) and diacylglycerol (DAG). The M_1 receptors targeted in the aforementioned Hille group studies are not expressed in ventricular myocytes but several other G_q-coupled receptors are, including angiotensin type 1 receptors (AT1R). Activated by the peptide hormone and vasoconstrictor agonist angiotensin II (AngII) (23), the AT1R/G_q/PLC signaling cascade is triggered during acute blood pressure control and chronically during hypertension and heart failure (HF) where it is implicated in cardiac hypertrophy and fibrosis (24–26). While AngII and its derivative Ang(1-7) can act on other receptors in the heart including angiotensin type 2 receptors, and Ang(1-7)/Mas receptors (27), we focus here on the effects on AT1R since this is the only pathway of the three that is G_q-coupled and thus is the most likely to directly modulate PIP_2 levels.

AngII has both indirect and direct effects on the heart. Indirectly, the effects of AngII on the vasculature change hemodynamic loading conditions. Directly, AngII has been demonstrated to affect cardiomyocyte L-type Ca^{2+} channel currents (I_{Ca}) in a species-dependent manner. Accordingly, the regulation of cardiac $Ca_V1.2$ by acute AngII treatment has been varyingly reported to cause an increase (in rabbit, cat, and cultured neonatal rat) (28–30), or a decrease in (human, chick, and cultured neonatal rat) (6, 31, 32) cardiomyocyte I_{Ca}. However, the underlying mechanism is unclear. Some have implicated channel phosphorylation by protein kinase C (PKC) as the regulatory driver (32, 33), while others have suggested a role for arachidonic acid and a $Ca_V\beta$ isoform-dependent effect (31). Thus, a unifying theory that explains the I_{Ca}-depleting effects of AngII on cardiomyocytes remains elusive and is the focus of this study.

We hypothesize that PIP_2 depletion is the driver of the regulatory effects of AngII on cardiac $I_{Ca.}$ Furthermore, we propose that PIP_2 stabilizes $Ca_V1.2$ channel expression in the t-tubule sarcolemma and that AngII can acutely depress cardiac excitability by stimulating PIP_2 depletion which destabilizes PM $Ca_V1.2$ and ultimately leads to their removal from the PM. Using electrophysiology, total internal reflection fluorescence (TIRF) microscopy and single-molecule localization microscopy, biochemistry, and lipid mass spectrometry approaches, our investigation uncovered a novel consequence of AngII signaling, that acute physiological signaling through AngII and the induction of PIP_2 depletion results in destabilization of PM $Ca_V1.2$ channels, triggering their removal and the acute reduction of I_{Ca} and contractility in the heart.

Results

Receptor-Stimulated PIP_2 Depletion Destabilizes PM Expression of $Ca_V1.2$ Channels. We began our study by testing the hypothesis that PIP_2 stabilizes $Ca_V1.2$ channel expression in the PM (as illustrated in Fig. 1*A*) by examining the effects of G_q-coupled receptor-driven PIP_2 depletion on PM $Ca_V1.2$ channel expression in a reductionist system lacking the complexities of a cardiomyocyte. Accordingly, fluorescence imaging experiments were performed on tsA201 cells transfected with M_1R or AT1R. Cells were additionally transfected with a red fluorescent protein tagged PIP_2 probe based on the pleckstrin homology domain of PLC [PH-PLC∂1-RFP (34)], and a cyan fluorescent protein (CFP) tagged $Ca_V1.2$ ($Ca_V1.2$-CFP) to monitor PM PIP_2 and channel expression, respectively. Adapting the approach of Suh et al. (17), M_1R were activated with a saturating concentration of the agonist Oxo-m (10 μM), triggering the G_q/PLC signaling pathway and resulting in PIP_2 hydrolysis. In TIRF time series experiments application of Oxo-m triggered a robust 48.1 ± 4.7% depletion of $PH_{PLC\partial1}$-RFP from the PM, which upon washout was recovered, demonstrating PIP_2 hydrolysis and resynthesis (Fig. 1 *B* and *C*). A 22.4 ± 3.1% decline in PM $Ca_V1.2$-CFP commenced within ~10 s of PIP_2 depletion followed by a partial recovery upon washout (Fig. 1 *D* and *E*). This delay potentially reflects the time required for channel endocytosis and recycling to begin after PIP_2 depletion. Once initiated, the channel removal and recovery phases followed a similar kinetic profile to that of the PH-fluoroprobe (channel: $\tau_{depletion}$ = 49.24 ± 4.54 s, $\tau_{recovery}$ = 118.92 ± 6.16 s; PIP_2: $\tau_{hydrolysis}$ = 21.67 ± 1.85 s, $\tau_{recovery}$ = 139.46 ± 6.83 s). These PIP_2 kinetics measurements agree with prior published values following M_1R activation in tsA201 cells (35, 36). In AT1R expressing tsA201 cells, the application of AngII (100 nM) resulted in a 39.6 ± 3.6% depletion of $PH_{PLC\partial1}$-YFP signals (PIP_2 $\tau_{hydrolysis}$ = 40.15 ± 17.20 s). This was accompanied by an 11.1 ± 1.6% decline in PM $Ca_V1.2$-CFP that began ~30 s after the onset of PIP_2 depletion (Fig. 1 *F*–*I*). Taken together, these experiments indicate that $Ca_V1.2$ channel destabilization and removal from the PM occurs after G_qPCR/PLC-mediated PIP_2 hydrolysis.

Recruitment of a Lipid Phosphatase to the PM Leads to $Ca_V1.2$ Endocytosis. G_q-coupled receptor signaling cascades generate/activate several second messengers and downstream effectors, e.g., arachidonic acid and protein kinase C (PKC), that could themselves affect $Ca_V1.2$ channel expression. To isolate the specific effects of PIP_2 depletion on PM $Ca_V1.2$ expression levels, we utilized a chemical dimerization strategy to deplete PIP_2 in a targeted manner that would be independent of receptor signaling. In this previously described system, addition of rapamycin is used to dimerize an FKBP-rapamycin binding (FRB) domain-linked membrane anchor (Lyn_{11}-FRB), to an FK506 binding protein (FKBP) that is coupled to a 4′, 5′ lipid phosphatase enzyme (FKBP-4′ 5′ phosphatase) (37). This irreversible dimerization recruits cytosolic FKBP-4′, 5′ phosphatase to the PM anchor where it removes the 4′ and 5′ phosphate groups from PIP_2 to produce PI (Fig. 2*A*). To control for any rapamycin-specific effects, we initially recruited an enzymatically dead lipid phosphatase to the PM of transfected tsA201 cells and observed no reduction in green fluorescent protein (GFP) tagged $Ca_V1.2$ ($Ca_V1.2$-GFP) (Fig. 2 *B* and *C*). In contrast, PM recruitment of a catalytically active phosphatase produced a 12.4 ± 1.7% reduction in PM $Ca_V1.2$-GFP in response to rapamycin-induced PIP_2 depletion (Fig. 2 *D* and *E*). Together, these experiments show that PIP_2 depletion destabilizes PM expression of $Ca_V1.2$-GFP.

PIP_2 Depletion Triggered $Ca_V1.2$ Endocytosis Is Dynamin-Dependent. AT1R are known to undergo agonist-promoted internalization in a process that involves β-arrestin and dynamin-dependent endocytosis of the receptors (38). Thus to determine whether AngII-stimulated internalization of $Ca_V1.2$-GFP occurred simply due to receptor-adjacent channels being caught up in AT1R sequestration, we stimulated the receptors with [Sar1,Ile4,Ile8]-AngII (SII-AngII), a β-arrestin-biased agonist of AT1R (39). SII-AngII binding to AT1R induces β-arrestin recruitment but fails to engage G-proteins thus allowing discrimination between an internalization that requires β-arrestin and one that is stimulated by G_q signaling (Fig. 3*A*). In proof-of-reagent experiments, confocal imaging performed on AT1R-mCherry and $PH_{PLC\partial1}$-CFP expressing tsA201 cells revealed AT1R-mCherry internalization in response to SII-AngII (Fig. 3*B*), but PIP_2 depletion only occurred during AngII application (Fig. 3 *C* and *D*). As PIP_2

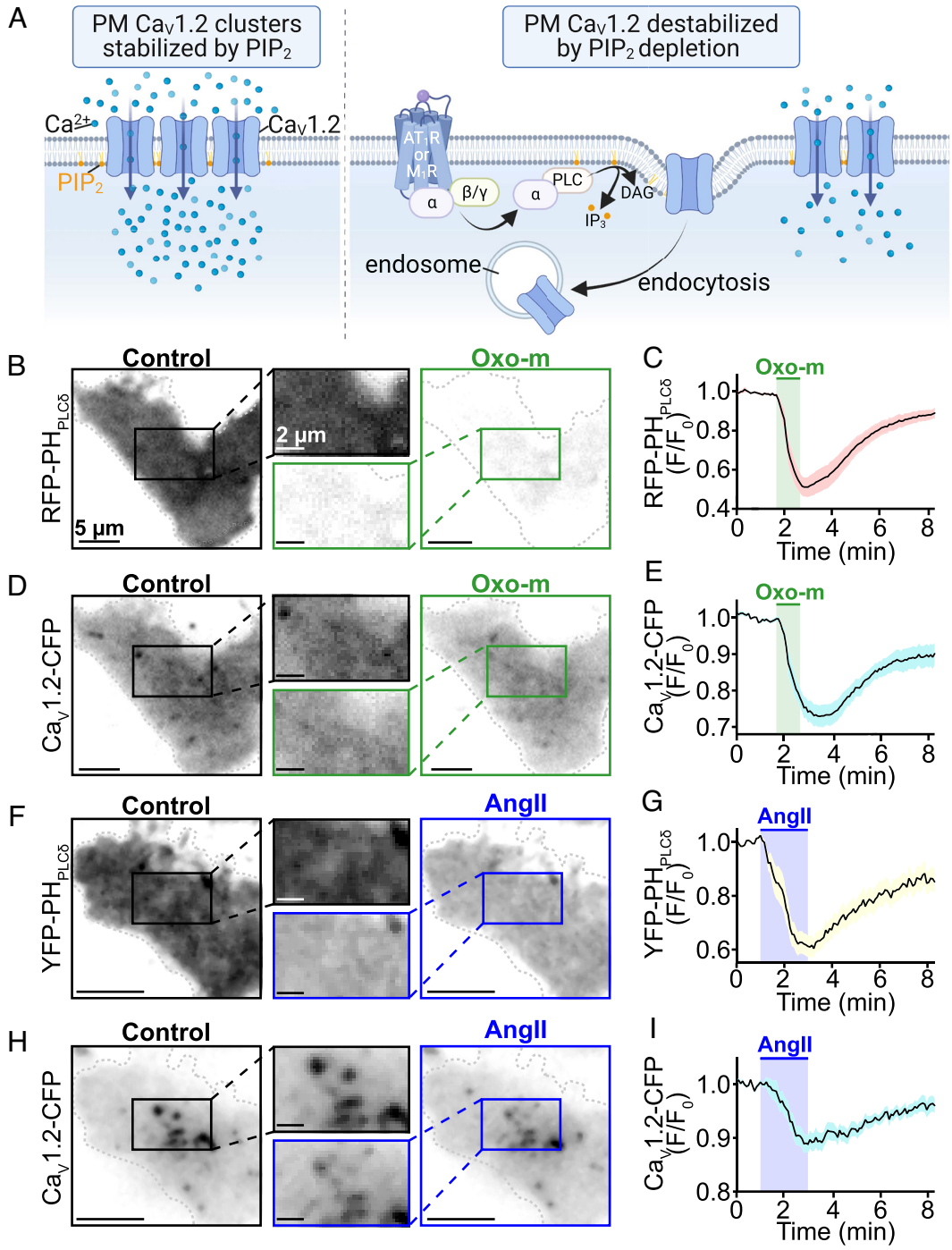

Fig. 1. Receptor-stimulated PIP_2 depletion destabilizes plasma membrane $Ca_V1.2$ expression. (*A*) Illustration of our hypotheses where PIP_2 stabilizes membrane expression of $Ca_V1.2$ (*Left*) and G_q-coupled receptor-stimulated PIP_2 hydrolysis destabilizes $Ca_V1.2$ expression triggering their endocytosis (*Right*). (*B*) Representative TIRF images showing localization of the PIP_2 biosensor RFP-PH-PLC∂1 before and after 10 μM Oxo-m treatment in M_1R and $Ca_V1.2$-expressing tsA201 cells ($n = 12$). (*C*) Time-course (mean ± SEM) of the Oxo-m stimulated changes in normalized RFP-PH-PLC∂1 fluorescence emission (F/F_0) in the TIRF footprint. (*D*) TIRF images of $Ca_V1.2$-CFP in the same cell before and after Oxo-m, and (*E*) the average time-course of changes in $Ca_V1.2$-CFP fluorescence emission (F/F_0) over the course of the experiments. (*F*) Representative TIRF images and (*G*) average time-course of intensity changes of YFP-PH-PLC∂1 before and after 100 nM AngII treatment in AT1R and $Ca_V1.2$-expressing tsA201 cells ($n = 13$). (*H*) TIRF images of $Ca_V1.2$-CFP in the same cell and, (*I*) average time-course of the experiments.

hydrolysis occurred, $PH_{PLC\partial1}$-CFP lost its binding partner in the PM, was released from membrane sites and in turn accumulated in the cytosol. These results illustrate the β-arrestin bias of SII-AngII and its failure to engage G-proteins. Importantly, TIRF experiments on cells expressing $Ca_V1.2$-GFP revealed no change in TIRF fluorescence of the channel with the SII-AngII treatment. Moreover, after a washout period, these same cells responded to AngII, leading to a 12.7 ± 2.3% reduction in channel fluorescence (Fig. 3*E*). Collectively, these results indicate that AngII-stimulated $Ca_V1.2$ channel internalization does not occur due to β-arrestin-dependent sequestration of neighboring AT1R.

Next, to test the hypothesis that AngII-stimulated $Ca_V1.2$ channel endocytosis was dynamin-dependent (*SI Appendix*, Fig. S1), we pre-treated $Ca_V1.2$-GFP and AT1R expressing tsA201 cells with the dynamin inhibitor dynasore (80 μM). In TIRF imaging experiments, this treatment prevented AngII-stimulated $Ca_V1.2$ removal from the PM (Fig. 3*F*). The washout of dynasore and subsequent reapplication of AngII to the same cells revealed the

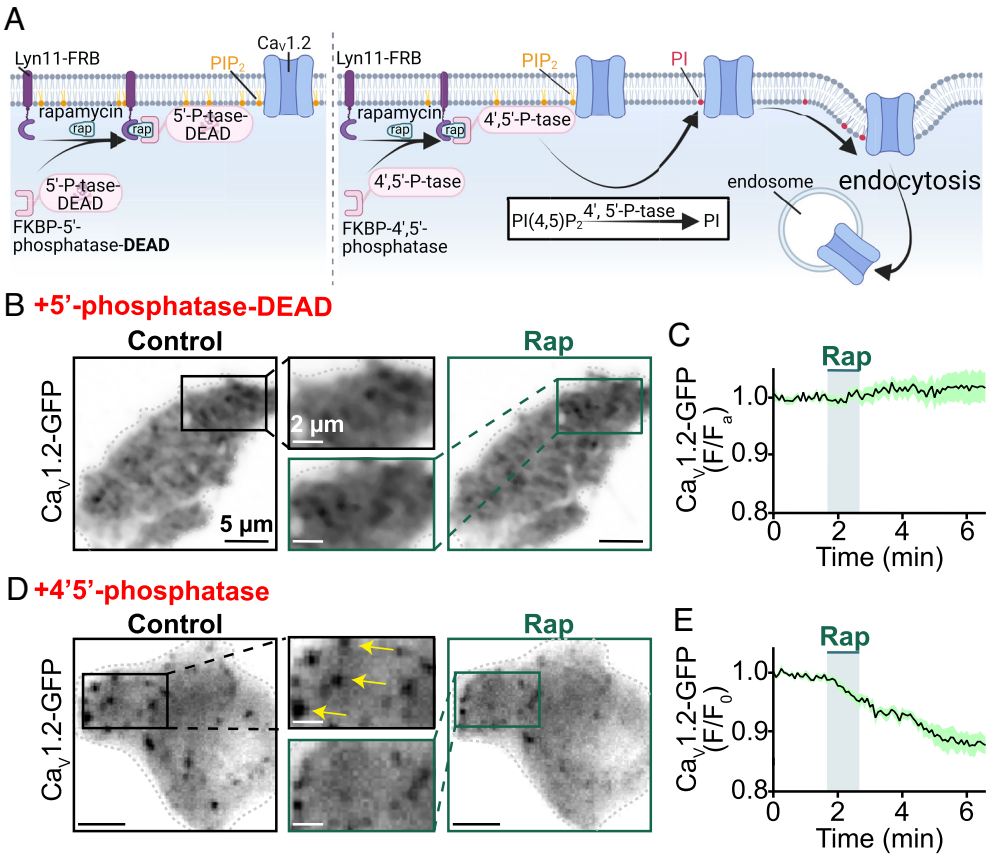

Fig. 2. Receptor-independent PIP_2 depletion via chemical translocation of a lipid phosphatase destabilizes plasma membrane $Ca_V1.2$ expression. (*A*) Illustration of the FKBP–FRB rapamycin-dependent dimerization system used to irreversibly recruit an enzymatically dead (control; *Left*) or an active (*Right*) lipid phosphatase to the PM. The active enzyme depletes PIP_2 by metabolizing it into PI. The cartoon graphically illustrates the testable prediction that this would destabilize PM expression of $Ca_V1.2$ and trigger their endocytosis. (*B*) TIRF images and (*C*) average $Ca_V1.2$-GFP (F/F_0) time-course showing PM $Ca_V1.2$-GFP expression in transfected tsA201 cells before and after rapamycin (1 μM) induced recruitment of enzymatically dead 5′-lipid-phosphatase (n = 7). (*D*) TIRF images and (*E*) average $Ca_V1.2$-GFP (F/F_0) time-course showing modulation of PM $Ca_V1.2$-GFP expression in transfected tsA201 cells before and after rapamycin-induced recruitment of active 4′,5′-phosphatase (pseudojanin-FKBP; n = 6).

recovery of the $Ca_V1.2$ channel removal response (Fig. 3*F*). Channel endocytosis was determined to be Ca^{2+} independent, as it persisted when Ba^{2+} was substituted for Ca^{2+} (*SI Appendix*, Fig. S2). These results confirm that AT1R-stimulated PIP_2 depletion destabilizes $Ca_V1.2$ anchoring in the PM and triggers dynamin-dependent endocytosis of the channel in tsA201 cells.

AngII Reduces $Ca_V1.2$ Cluster Size and Sarcolemma Expression in Ventricular Myocytes. Turning our attention to primary cells from native tissues, we set out to determine whether a similar AngII-triggered $Ca_V1.2$ endocytosis exists in freshly isolated ventricular myocytes. If a similar phenomenon exists in these cells, then a testable prediction is that acute treatment with AngII should reduce $Ca_V1.2$ channel expression at the sarcolemma. That hypothesis was rigorously tested using a two-pronged approach. First, we examined the nanoscale distribution of immunostained $Ca_V1.2$ channels using super-resolution single molecule localization microscopy (SMLM). $Ca_V1.2$ channel cluster areas in myocytes acutely treated with AngII were 30.9 ± 4.4% smaller on average compared to controls (Fig. 4 *A* and *B*). The number of events per pixel within the cell-occupied area of the localization map provides an indication of the density of labeling and the number of channels. This measure was also reduced by 47.9 ± 14.8% in the AngII-treated cells versus controls (Fig. 4*C*) suggesting that acute AngII treatment reduced the number of $Ca_V1.2$ channels in the t-tubule sarcolemma. Similar results were obtained from female ventricular myocytes suggesting this response is conserved across both sexes (*SI Appendix*, Fig. S3). It is also noteworthy that this stimulated decrease in $Ca_V1.2$ channel clustering and expression appears confined to the t-tubules as crest-localized $Ca_V1.2$ clusters were not significantly altered by acute AngII (*SI Appendix*, Fig. S4).

Next, in the second prong of our approach, we biotinylated membrane proteins from isolated myocytes and quantified the biotinylated (plasma membrane-localized) fraction of the $a_1$1.2 $Ca_V1.2$ channel subunit that bound to NeutrAvidin beads in pull-down assays via immunoblotting. Here we determined that surface $a_1$1.2 in the AngII-treated myocytes was reduced by 58.8 ± 13.8% in comparison to controls (Fig. 4 *D* and *E*). Altogether, these complementary results using two separate techniques reveal that acute treatment of mouse ventricular myocytes with AngII leads to reduced expression of $Ca_V1.2$ channels at the PM.

Whole-Heart Phospholipid Species' Levels Are Altered by Acute AngII Treatment. To establish that AT1R/G_q/PLC-driven PIP_2 depletion drives these changes in $Ca_V1.2$ channel distribution, it was necessary to quantify phosphoinositide species in hearts with and without acute AngII-treatment. A simplified view of phosphoinositide metabolism is shown in Fig. 4 *F*, *Top*. We measured each of these species using phospholipid mass spectrometry and found that Langendorff perfusion of hearts with 100 nM AngII for just 5 min generated significant alterations in the levels of PIP_2 and its precursor PIP (Fig. 4 *F*, *Bottom*). Specifically, we observed a 62.8 ± 22.4% decrease in PIP and a 44.2 ± 13.0% decrease in PIP_2 (Fig. 4 *F*, *Bottom*) after AngII.

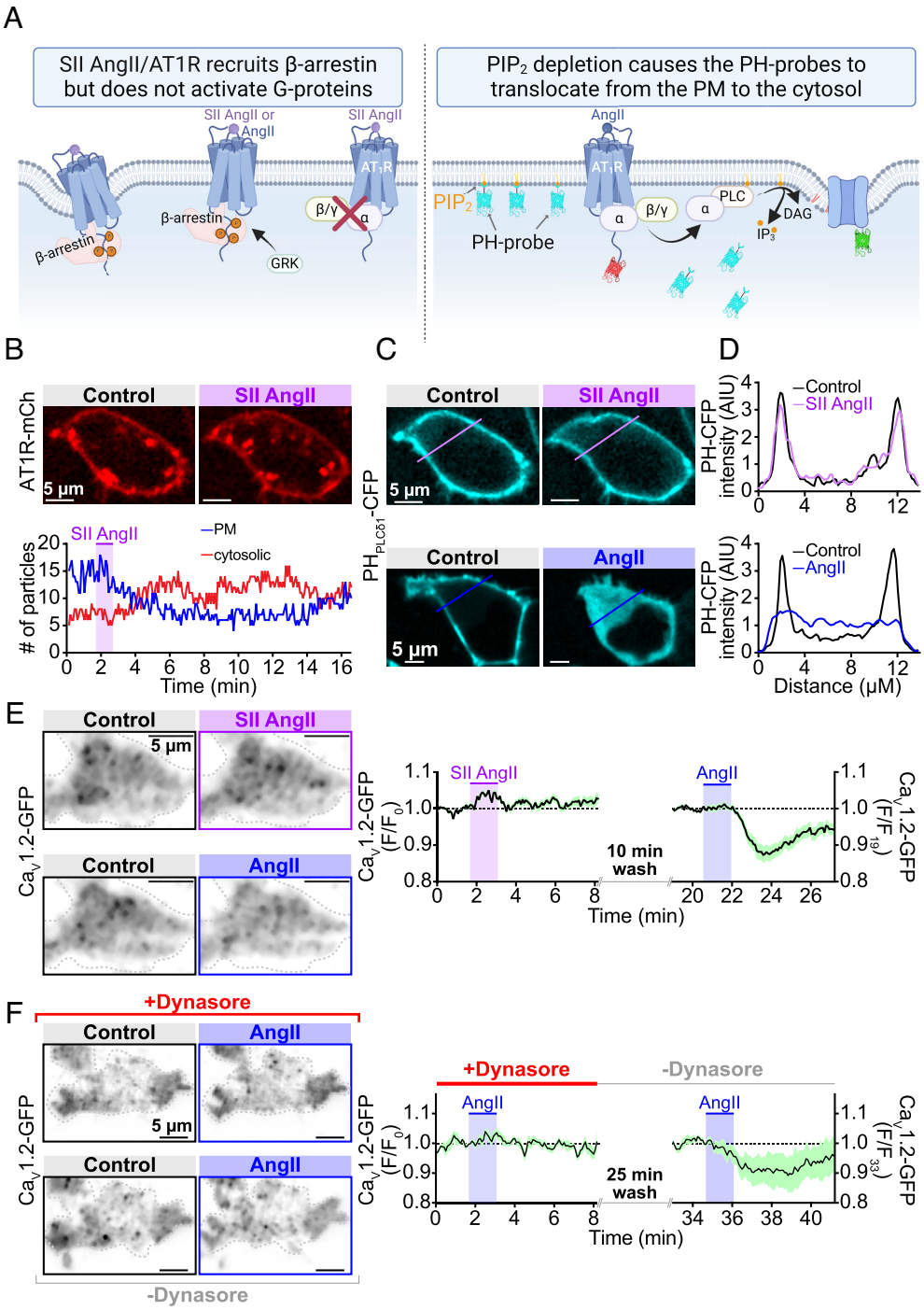

Fig. 3. AngII/AT1R stimulated $Ca_V1.2$ endocytosis is dependent on dynamin, not β-arrestin. (*A*) Illustration of our experimental design where SII AngII was used to stimulate β-arrestin recruitment but failed to activate G-proteins (*Left*). (*Right*) CFP-tagged PH-probes were used to monitor PM PIP_2 levels, while $Ca_V1.2$-GFP and AT1R-mCherry were used to track the localization of the channels and receptors before and after application of agonists. (*B*, *Top*) Representative confocal images showing AT1R-mcherry localization in tsA201 cells, and (*Bottom*) accompanying time-course showing AT1R-mCherry "particle" tracking in the PM (blue line) and cytosolic (red line) compartments of this cell before and after application of the β-arrestin-biased AT1R agonist, SII AngII (10 μM; $n = 8$). (*C*) Confocal images showing localization of the PIP_2 biosensor PH-PLCδ1-CFP before and during application of SII AngII (*Top*), or AngII (*Bottom*). (*D*) Plot profiles of normalized PH-PLCδ1-CFP fluorescence intensity across the cell in each condition at the line-regions of interest (ROIs) indicated in panel *C*. (*E*) TIRF images showing $Ca_V1.2$-GFP localization in a representative tsA cell treated first with SII AngII, and subsequently with 100 nM AngII. (*Right*) Corresponding mean ± SEM time courses of the normalized $Ca_V1.2$-GFP intensity ($n = 14$). (*F*) Representative TIRF images and corresponding mean ± SEM time-courses showing $Ca_V1.2$-GFP intensity in tsA201 cell TIRF footprints during application of AngII in the presence (*Top*), and absence (*Bottom*) of the dynamin-inhibitor dynasore (10 μM; $n = 5$).

These results suggest that acute, physiological elevations in AngII in the heart result in PIP and PIP_2 depletion.

AngII-Stimulated $Ca_V1.2$ Endocytosis in Cardiomyocytes Requires PIP_2 Depletion. To address the question of whether the reductions in t-tubule sarcolemma-localized $Ca_V1.2$ were driven by PIP_2 depletion-triggered endocytosis, SMLM was performed on cardiomyocytes supplemented with PIP_2. We reasoned that if PIP_2 stabilizes $Ca_V1.2$ channel expression then boosting PIP_2 concentration in the membrane might reduce or eliminate the AngII-stimulated endocytosis. In line with that prediction, PIP_2 supplementation prevented AngII-mediated decreases in cluster

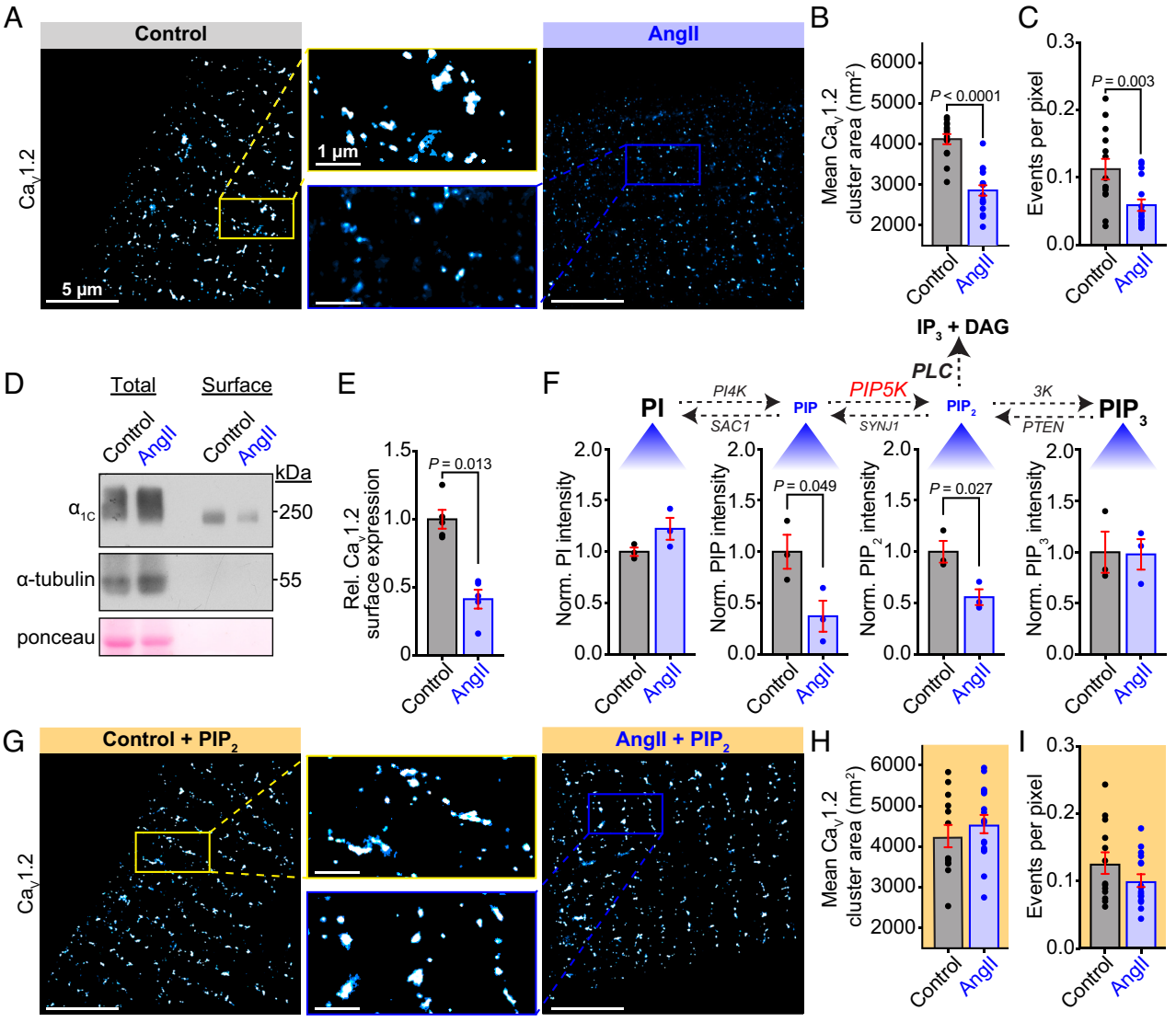

Fig. 4. Acute AngII application reduces t-tubular Ca$_V$1.2 cluster area and PM expression in a PIP$_2$-depletion–dependent manner. (*A*) Representative SMLM localization maps showing Ca$_V$1.2 channel distribution in the t-tubules of mouse ventricular myocytes with (*Right*) or without (*Left*) AngII-stimulation. Boxes indicate the location of the enlarged regions. (*B*) Aligned dot plots showing mean Ca$_V$1.2 channel cluster areas, and (*C*) events per pixel as an indicator of channel expression density (control: $N = 4$, $n = 14$; AngII: $N = 3$, $n = 17$). (*D*) Representative western blot image of the total and biotinylated cell surface fraction of Ca$_V$1.2, internal control alpha-tubulin, and total protein ponceau stain, in untreated control, and AngII-treated ventricular myocyte lysates. (*E*) Aligned dot plots showing relative Ca$_V$1.2 surface expression ($N = 13$, $n = 5$). (*F, Top*) The homeostatic phospholipid metabolism pathway with species scaled to illustrate the observed effects of AngII. (*Bottom*) Histograms summarizing UPLC-MS/MS measurements of PI, PIP, PIP$_2$, and PIP$_3$ in samples of untreated control or AngII-stimulated whole heart lysates, ($N = 3$ for each). (*G*) SMLM localization maps showing Ca$_V$1.2 channel distribution in control and AngII-treated myocytes supplemented with PIP$_2$ (control + PIP$_2$ $N = 3$, $n = 13$; AngII + PIP$_2$ $N = 3$, $n = 16$). (*H*) Aligned dot plots showing mean Ca$_V$1.2 channel cluster area and (*I*) the events per pixel in each condition. Error bars indicate SEM. Statistical analyses on data summarized in *B*, *C*, *F*, *H*, and *I* were performed using unpaired, two-tailed Student's *t*-tests. Data in *E* were compared using a paired, two-tailed Student's *t*-test.

area and expression (Fig. 4 *G–I*). Furthermore, myocyte treatment with the β-arrestin-biased AT1R agonist SII-AngII failed to trigger the endocytosis response (*SI Appendix*, Fig. S5). As discussed above, SII-AngII bound AT1R cannot engage G-proteins to activate PLC-mediated hydrolysis of PIP$_2$, thus these results reinforce the idea that AngII stimulation of AT1R triggers Ca$_V$1.2 channel endocytosis in a process that requires PIP$_2$ depletion.

Ca$_V$1.2 Channels Endocytosed Downstream of AT1R Activation Are Stored in Endosomes. We next sought to visualize the dynamics of AngII-stimulated Ca$_V$1.2 endocytosis in live cells. To accomplish this, we utilized transduced myocytes isolated from mice 2 wk after their inoculation with a retro-orbital injection of the AAV9-Ca$_V$β$_2$a-paGFP. The transduced expression construct encodes an auxiliary subunit that finds and binds endogenous pore-forming α$_{1C}$-subunits on a 1:1 basis and thus acts as a fluorescent biosensor of Ca$_V$1.2 channels as has been extensively verified in other studies (4, 5). After photoactivation with 405 nm light, clusters of GFP-tagged channels were visualized and a time series of experiments was performed to track biosensor-tagged channels before and during application of AngII via 150 nm penetration depth TIRF microscopy, an imaging technique that allows detection of the surface and initial portion of the t-tubule sarcolemma. Image analysis was used to identify and quantify subpopulations of channels that were inserted, removed, or static during AngII treatment relative to the control period (Fig. 5 *A* and *B*). Our results indicated a strong bias toward channel removal during AngII treatment (Fig. 5*B*). Since the population of channels at the membrane at any given time is dictated by the balance between their insertion and removal, enhanced removal

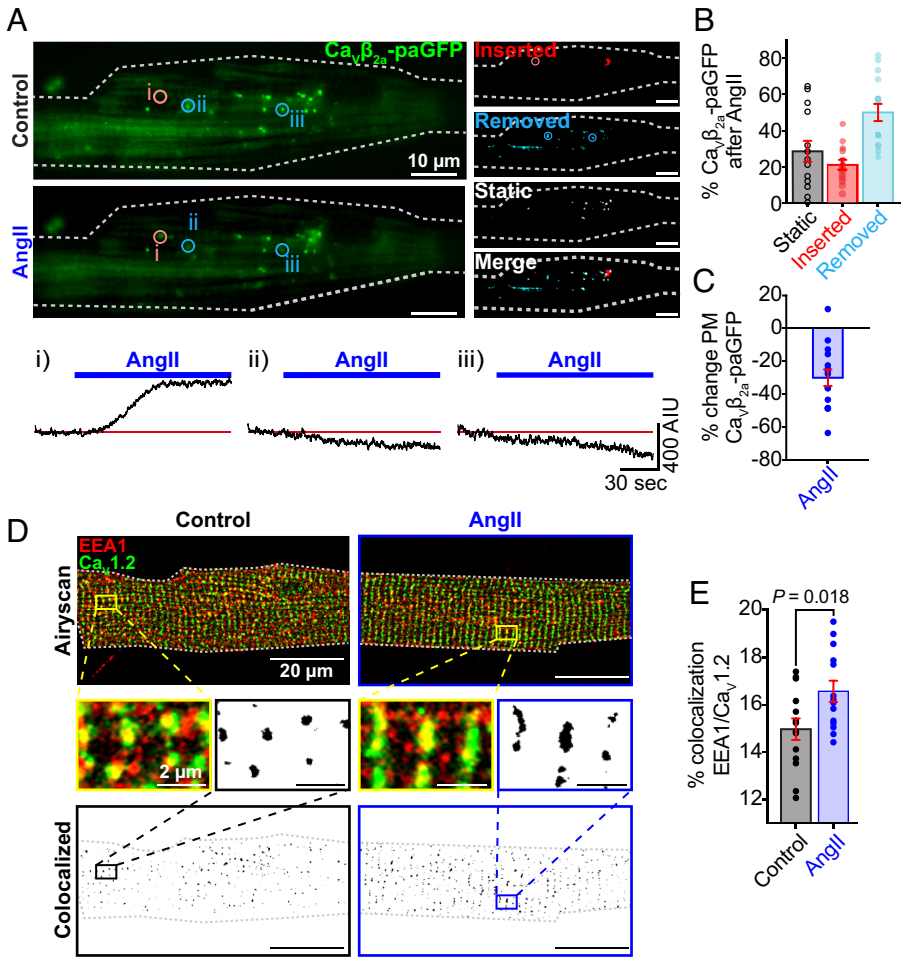

Fig. 5. AngII promotes $Ca_V1.2$ channel removal from cardiomyocyte sarcolemmas and sequestration in early endosomes. (*A*) Representative TIRF images of GFP fluorescence emission from $Ca_V\beta_{2a}$-paGFP transduced cardiomyocytes before (*Top*) and after 100 nM AngII (*Bottom*) ($N = 5$, $n = 14$). Images illustrating stable, inserted, and endocytosed channel populations are shown to the *Right*. Time courses of the changes in $Ca_V\beta_{2a}$-paGFP intensity in individual ROIs (indicated by circles on TIRF images) are represented below. (*B* and *C*) Histograms summarizing the percentage of static, inserted, and removed channel populations after AngII (*B*) and the percentage change of TIRF-footprint $Ca_V\beta_{2a}$-paGFP fluorescence after AngII (*C*). (*D*) Two-color Airyscan super-resolution images showing distributions of $Ca_V1.2$ and $EEA1^+$ early endosomes in representative control (*Left*) and AngII-stimulated (*Right*) myocytes. Binary colocalization maps (*Bottom*) display pixels in which $Ca_V1.2$ and endosomal expression fully overlap. (*E*) Histogram summarizing the percentage colocalization between EEA1 and $Ca_V1.2$ in control ($N = 3$, $n = 14$) and AngII-stimulated ($N = 3$, $n = 13$) conditions. Statistical analyses on data summarized *E* was performed using unpaired, two-tailed Student's *t*-tests. Error bars indicate SEM.

relative to insertion will lead to reduced expression of channels at the membrane. Accordingly, we found a 28.8 ± 5.2% reduction in biosensor-tagged channels in the TIRF footprints of myocytes after AngII (Fig. 5*C*). This evident dynamic shift toward channel internalization invites the question, where are these channels going?

Based on our prior work (4), we hypothesized that internalized channels may populate an endosomal reservoir. To determine the acute fate of these channels in response to AngII, we examined the distribution of $Ca_V1.2$ on EEA1-positive early endosomes, Rab7-positive-late endosomes, and Rab11-positive recycling endosomes. Two-color Airyscan super-resolution images were taken on control or AngII-treated AMVMs immunostained for $Ca_V1.2$ and these endosomal markers. Colocalization analysis revealed a 10.7 ± 4.2% increase in $Ca_V1.2$ localized on early endosomes treated with AngII (Fig. 5 *D* and *E*). However, there was no significant difference in the percent of $Ca_V1.2$ on recycling endosomes (*SI Appendix*, Fig. S6 *A* and *B*) and late endosomes (*SI Appendix*, Fig. S6 *C* and *D*) between the two groups. This suggests that after only 5 min of AngII signaling, internalized channels are gathered on early endosomes but have not yet been shuttled toward recycling or degradation pathways.

AngII Attenuates I_{Ca}, PIP_2, and Ca^{2+} Transient Amplitudes in Cardiomyocytes. We hypothesized that the apparent deficit in PM $Ca_V1.2$ channel expression and clustering would ultimately decrease functional output. To test that, we performed perforated patch clamp experiments and recorded I_{Ca} from freshly isolated myocytes, before and during acute AngII-treatment. Accordingly, application of AngII caused an ~20% decrease in I_{Ca} density that occurred with a τ of 0.69 min (Fig. 6 *A* and *B*). If this AngII-induced current reduction is triggered by PIP_2 depletion and destabilization of $Ca_V1.2$, then a testable prediction is that PIP_2 hydrolysis should occur on a similar timescale. To test this, we transduced ventricular myocytes with adenovirus-packaged RFP-$PH_{PLC\delta1}$. After 48 h in culture, the transduced PH-probe biosensor was predominantly localized to the sarcolemma of the cardiomyocytes (Fig. 6*C*). Time series confocal experiments revealed an AngII-induced reduction in membrane localization of RFP-$PH_{PLC\delta1}$ due to PIP_2 hydrolysis and a subsequent recovery upon washout as PIP_2 was resynthesized (Fig. 6*D*). The τ of PIP_2 hydrolysis was, at 0.42 min, slightly faster than that of the AngII-triggered current reduction. Superimposition of the current decay onto the PH-probe measurements revealed the initiation of PIP_2 hydrolysis slightly precedes the onset of I_{Ca} decay.

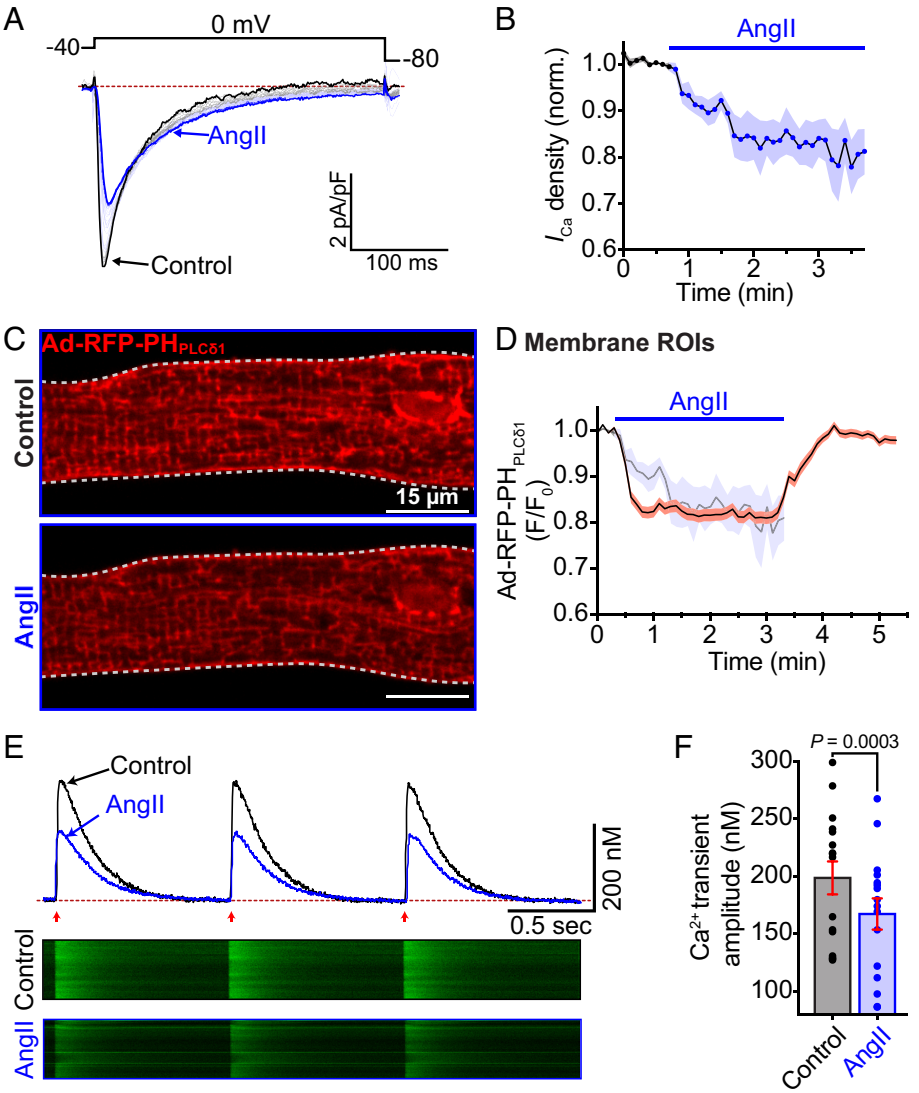

Fig. 6. AngII depression of ventricular myocyte $Ca_V1.2$ currents and Ca^{2+} transient amplitude occurs coincidently with PIP_2 depletion. (*A*) Representative L-type I_{Ca} elicited every 6 s by a 300 ms depolarization step from −40 mV to 0 mV. Black traces show the current before, and blue traces the current after AngII. (*B*) Diary plot of normalized Ca^{2+} current density summarizing the results from $N = 4$, $n = 6$ cells. (*C*) Confocal images of a cardiomyocyte transduced with Ad-RFP-$PH_{PLC\delta1}$ before and during AngII. (*D*) Time course of the changes in membrane RFP-$PH_{PLC\delta1}$ intensity (F/F_0) in the same cell before, and during AngII and its recovery on washout. Representative of $N = 3$, $n = 4$ cells. Time course of the changes in I_{Ca} from panel *B* are superimposed for ease of comparison. (*E*) Representative EFS-evoked Ca^{2+} transients recorded under control (black traces) and AngII-stimulated conditions (blue traces). Arrows indicate EFS pulse application at 1 Hz. Corresponding line scans from the fluo4-AM-loaded cells appear below. (*F*) Histogram summarizing Ca^{2+} transient amplitude ($N = 3$, $n = 16$). Data were analyzed using paired Student's *t*-tests. Error bars indicate SEM.

Finally, to investigate the effects of AngII on EC-coupling, we recorded Ca^{2+} transients from freshly isolated myocytes, before and during acute AngII-treatment. Accordingly, AngII elicited a a 15.8 ± 3.3% reduction in EFS-stimulated Ca^{2+} transient amplitude (Fig. 6 *E* and *F*). In line with our hypothesis, these data collectively show that acute AngII-stimulation tunes and diminishes EC-coupling and does so on a timescale that closely aligns with that of PIP_2 hydrolysis.

Discussion

Our data show that PIP_2 stabilizes cardiac $Ca_V1.2$ channel PM lifetime and that AngII-induced PIP_2 depletion destabilizes PM $Ca_V1.2$ clusters, triggers their dynamin-dependent endocytosis, results in the acute reduction of whole-cell I_{Ca}, and decreases Ca^{2+} transient amplitudes, which diminishes myocardial excitability and contractility. We provide evidence for this phenomenon using both a heterologous expression system and primary ventricular myocytes. In transfected tsA201 cells, both G_qPCR-mediated and receptor-independent PIP_2 depletion triggered $Ca_V1.2$ removal from the PM. In myocytes, AngII/AT1R signaling triggered sarcolemmal PIP_2 hydrolysis, reduced $Ca_V1.2$ expression and cluster area, and resulted in the stimulated removal of $Ca_V1.2$ from the PM to early endosomes. PIP_2 reinforcement stabilized $Ca_V1.2$ channel clusters and their sarcolemmal expression. β-arrestin biased AT1R agonism also eliminated this response, specifically implicating G_q activation. Moreover, dynamin inhibition abrogated the internalization response, suggesting internalization proceeded via dynamin-dependent endocytosis.

The finding that $Ca_V1.2$ endocytosis is dynamin-dependent agrees with published work from several other groups although none were testing the triggering of this event by AngII-mediated PIP_2 depletion (12, 40, 41). In our hands, endocytosed $Ca_V1.2$ were sequestered into early endosomes but not recycling or late endosomes. Previous work from our group identified an endosomal reservoir of $Ca_V1.2$ channels on early and recycling endosomes

that can be mobilized to the t-tubule sarcolemma of cardiomyocytes during periods of acute stress via Rab4-dependent fast and Rab11-dependent slow recycling pathways (4), enhancing $Ca_V1.2$ cluster areas and channel expression in t-tubule sarcolemma (5), and facilitating a positive inotropic response to tune cardiac performance to meet physiological demands. Results from the current study reveal activation of AT1R has essentially the opposite effect, invoking an image of a rheostatic system whereby cardiac EC-coupling can be tuned up or down by manipulating sarcolemmal expression of $Ca_V1.2$ channels via selective activation of different receptor populations. While our work rules out the possibility that the acute $Ca_V1.2$ internalization response we report occurs due to their entrapment in β-arrestin-dependent sequestration of nearby AT1R, others have shown that longer, 1 h applications of AngII produce $Ca_V1.2$ internalization that does involve β-arrestin (6). We found that AngII-stimulated $Ca_V1.2$ internalization occurred predominantly in t-tubules and not in the sarcolemma crest. It is possible that AT1R are more closely associated with t-tubule $Ca_V1.2$ channels than with crest populations, creating signaling microdomains. However, to our knowledge, there are no specific antibodies against AT1R and thus this idea remains speculative.

Prior studies have indicated that neuronal $Ca_V1.2$ channel endocytosis occurs upon Ca^{2+} influx through the channels as the incoming Ca^{2+} binds to calmodulin (CaM) forming Ca^{2+}. CaM that competes with α-actinin for a common binding site on the α_{1C} C-terminal (12). In that model, binding of α-actinin to an α_{1C} surface-targeting motif promotes $Ca_V1.2$ channel expression on the PM. Ca^{2+}.CaM outcompetes α-actinin, displacing it from the channel and favoring endocytosis. Our model describes what appears to be a separate process since it occurs independently of Ca^{2+} influx, as shown by its persistence with Ba^{2+} substitution. We find that PIP_2 exerts a stabilizing influence on $Ca_V1.2$ surface expression and that its depletion by either G_q-receptor stimulation or PM recruitment of a lipid phosphatase favors channel endocytosis. This implies that PIP_2 must bind to the channel complex. Rosetta structural modeling has predicted the presence of at least one putative PIP_2 binding site formed by four arginines within the I-II loop α-helix region of $Ca_V1.2$ (42). Interestingly, neutralization of these residues removed PM binding of the linker and decreased on-gating current (Q_{on}), revealing that there were fewer functional channels at the PM. Thus, there appears to be a role for PIP_2 in supporting calcium channel activity and expression at the cardiac sarcolemma. Intriguingly, the putative site is found on the I-II loop that also contains the gain-of-function Timothy syndrome $Ca_V1.2$ mutation site at G406R (G436R in mice). Replacing a neutral glycine with a positively charged arginine might further enhance binding to negatively charged phospholipids at this interface. In our model, enhanced PIP_2 binding would favor stabilization of $Ca_V1.2$ channels at the PM and supporting that idea, we have previously reported that G436R mutant gain-of-function $Ca_V1.2$ channels form extremely large, pronounced clusters in ventricular myocytes (43). In $Ca_V2.2$ channels, high-resolution cryo-EM structures in the presence of a pore-blocking pain-killer called Ziconotide revealed a PIP_2 binding site that stabilizes the down conformation of voltage sensitive domain II (44). This would favor the closed state of the channel and limit Ca^{2+} influx. However, over 50% of the residues in that site are Ca_V2-specific, so it remains to be determined whether a homologous site exists in $Ca_V1.2$.

Our study provides a quantitative analysis of phosphoinositide species in the heart and reveals that PIP_2 levels measurably change during physiological G_q-protein coupled receptor signaling in cardiomyocytes. Specifically, we show that levels of PIP_2 and its precursor PIP are both significantly reduced by acute application of AngII. Further experiments on cultured adult mouse ventricular myocytes transduced with an adenovirus-packaged fluorescent PIP_2 biosensor (PH-RFP) revealed the kinetics of AngII-stimulated sarcolemmal PIP_2 depletion. The hydrolysis of PIP_2 was concordant with the observed reduction in I_{Ca} supporting the idea that PIP_2 depletion destabilizes $Ca_V1.2$ channels. The effects of G_q/PLC-dependent pathway activation were previously studied in guinea pig ventricular myocytes but in contrast to our results using different experimental approaches, the tested agonists (endothelin, phenylephrine, and adenosine) elicited no detectable change in total cardiac PIP_2 (45). Given that PIP_2 is a modulator of many cardiac ion channels and transporters including $Ca_V1.2$ (17), KCNQ1/E1 (46), K_{ATP} and Na^+-Ca^{2+} exchanger [NCX (47)], our findings have a broad impact. It remains to be determined whether PIP_2 exerts a similar stabilizing effect on $Ca_V1.2$ in other excitable tissues, including smooth muscle, neurons, and pancreatic islets. Specifically in the heart, elevated production of AngII is associated with cardiac hypertrophy, remodeling, and HF (48–51). Future studies should examine the effects of chronic AngII on phosphoinositide populations in the heart and the ramifications for cardiac ion channel function.

Our finding that PIP_2 depletion destabilizes $Ca_V1.2$ expression potentially explains prior results indicating voltage-gated Ca^{2+} channel current depletion by activation of M_1Rs or voltage-sensitive phosphatase (DR-VSP) (17, 20). In favor of this stabilization hypothesis, PIP_2 supplementation is known to reduce P/Q-type $Ca_V2.1$ channel rundown in *Xenopus* oocytes, while sequestering PIP_2 with antibodies increased rundown (19). Rundown describes the poorly understood process of ion channel current decline observed in whole-cell and excised-patch clamp recordings over time. The endocytosis of $Ca_V1.2$ channels from the membrane has also been proposed as a factor underlying rundown (12). The supplementation of patch bathing or cell dialyzing solutions with MgATP, CaM, or crude cytoplasmic extracts from cardiac cells (52) have all been reported to reduce I_{Ca} rundown (53, 54). MgATP supports PIP_2 resynthesis by activating lipid kinases (19, 46, 55), while Mg^{2+} can guard against PIP_2 hydrolysis by a charge shielding effect (56). CaM has also been reported to promote PIP_2 generation in cardiac cell membranes although the underlying mechanism underlying this effect is not understood (57). Accordingly, each of these additives support PIP_2 synthesis or maintenance and appear to stabilize $Ca_V1.2$ channel currents, supporting our hypothesis.

Prior studies have shown PIP_2 suppression of Ca_V currents dependent on the associated Ca_Vβ-subunit isoform with the palmitoylated $Ca_V\beta_{2a}$ conferring the least sensitivity to PIP_2 depletion (58). Our model implies the palmitoylation may provide an additional membrane anchor that stabilizes $Ca_V1.2$ and reduces its sensitivity to PIP_2 depletion. To that end, AngII inhibition of $Ca_V1.2$ currents has been shown to be less robust when co-expressed with $Ca_V\beta_{2a}$ versus other $Ca_V\beta$ subunits (31). In the heart, the most abundant isoform is $Ca_V\beta_{2b}$, a splice variant that lacks the consensus site for palmitoylation (59, 60) and thus cardiac $Ca_V1.2$ channels may be vulnerable to PIP_2 depletion. Dynamic imaging of $Ca_V\beta_{2a}$-paGFP transduced myocytes herein revealed a bias toward channel endocytosis with acute AngII-treatment but if palmitoylation of $Ca_V\beta_{2a}$ does in fact confer additional stability that reduces the modulatory effects of PIP_2 depletion on PM $Ca_V1.2$ expression levels, it is possible that these results represent an underestimation of the true effects in vivo.

In summary, our results show that PIP_2 stabilizes $Ca_V1.2$ channel expression at the PM and that acute AngII can depress cardiac EC-coupling by stimulating PIP_2 depletion and destabilization of

PM $Ca_V1.2$, leading to their endocytosis from the PM. Given that PIP_2 is present in every PM of every cell in the body, our findings have broad ramifications not only for cardiac physiology but for the myriad excitable cells that express $Ca_V1.2$.

Materials and Methods

All animal handling and procedures adhered to the NIH Guide for the Care and Use of Laboratory Animals (UC Davis) and were approved by the local Institutional Animal Care and Use Committee. Ventricular myocytes were isolated from 3 to 6-mo-old C57BL/6J mouse hearts via retrograde Langendorff perfusion as previously described (4, 5) and used in microscopy, Ca^{2+} transient, and/or patch-clamp electrophysiology experiments. In surface biotinylation experiments, isolated myocytes from untreated and AngII-treated hearts were biotinylated, lysed, and probed for protein content using western blot as previously described (61, 62). Phosphoinositide species were quantified using ultra-high-pressure liquid chromatography coupled to tandem mass spectrometry (UPLC-MS/MS) as previously described (63, 64). *N* and *n* represent the number of animals and number of cells, respectively. Data are reported as mean ± SEM. Datasets were compared using paired or unpaired Student's *t* tests, one-way ANOVAs, or two-way ANOVAs with Tukey's multiple comparisons post-hoc tests as stated in the figure legends. $P < 0.05$ was considered statistically significant. Detailed methods can be found in the *SI Appendix*.

Data, Materials, and Software Availability. All study data are included in the article and/or *SI Appendix*.

ACKNOWLEDGMENTS. Illustrations were generated using Biorender.com. This work was supported by NIH grants R01HL159304 and R01AG063796 to R.E.D. and R01GM127513 to E.J.D.; by T32 GM099608 and later American Heart Association Predoctoral Fellowship 827909 to T.L.V., by R25 GM056765 (Initiative for Maximizing Student Development) and T32 GM113770 to A.M.C. and by R01 NS123050, RF1 AG055357 and a WM Keck foundation award (to J.W.H.).

Author affiliations: [a]Department of Physiology and Membrane Biology, School of Medicine, University of California Davis, Davis, CA 95616; and [b]Department of Pharmacology, School of Medicine, University of California Davis, Davis, CA 95616

1. D. M. Bers, Cardiac excitation-contraction coupling. *Nature* **415**, 198–205 (2002).
2. M. B. Cannell, J. R. Berlin, W. J. Lederer, Effect of membrane potential changes on the calcium transient in single rat cardiac muscle cells. *Science* **238**, 1419–1423 (1987).
3. G. Liu *et al.*, Mechanism of adrenergic $Ca_V1.2$ stimulation revealed by proximity proteomics. *Nature* **577**, 695–700 (2020).
4. S. G. Del Villar *et al.*, Adrenergic control of sarcolemmal $Ca_V1.2$ abundance by small GTPase Rab proteins. *Proc. Natl. Acad. Sci. U.S.A.* **118**, e2017937118 (2021).
5. D. W. Ito *et al.*, beta-Adrenergic-mediated dynamic augmentation of sarcolemmal $Ca_V1.2$ clustering and co-operativity in ventricular myocytes. *J. Physiol.* **597**, 2139–2162 (2019).
6. T. Hermosilla *et al.*, Prolonged AT1R activation induces $Ca_V1.2$ channel internalization in rat cardiomyocytes. *Sci. Rep.* **7**, 10131 (2017).
7. M. A. Nystoriak *et al.*, Ser 1928 phosphorylation by PKA stimulates the L-type Ca^{2+} channel $Ca_V1.2$ and vasoconstriction during acute hyperglycemia and diabetes. *Sci. Signal.* **10**, eaaf9647 (2017).
8. T. Patriarchi *et al.*, Phosphorylation of $Ca_V1.2$ on S1928 uncouples the L-type Ca^{2+} channel from the beta2 adrenergic receptor. *EMBO J.* **35**, 1330–1345 (2016).
9. H. Tang, H. M. Viola, A. Filipovska, L. C. Hool, $Ca_V1.2$ calcium channel is glutathionylated during oxidative stress in guinea pig and ischemic human heart. *Free Radic. Biol. Med.* **51**, 1501–1511 (2011).
10. M. P. Tetreault *et al.*, Identification of glycosylation sites essential for surface expression of the $Ca_V\alpha_2\delta_1$ subunit and modulation of the cardiac $Ca_V1.2$ channel activity. *J. Biol. Chem.* **291**, 4826–4843 (2016).
11. W. Yuan, D. M. Bers, Ca-dependent facilitation of cardiac Ca current is due to Ca-calmodulin-dependent protein kinase. *Am. J. Physiol.* **267**, H982–993 (1994).
12. D. D. Hall *et al.*, Competition between alpha-actinin and Ca(2) (+)-calmodulin controls surface retention of the L-type Ca^{2+} channel $Ca_V1.2$. *Neuron* **78**, 483–497 (2013).
13. R. E. Dixon *et al.*, Graded Ca^{2+}/calmodulin-dependent coupling of voltage-gated $Ca_V1.2$ channels. *Elife* **4**, e05608 (2015).
14. C. M. Moreno *et al.*, Ca^{2+} entry into neurons is facilitated by cooperative gating of clustered $Ca_V1.3$ channels. *Elife* **5**, e15744 (2016).
15. J. P. Imredy, D. T. Yue, Mechanism of Ca^{2+}-sensitive inactivation of L-type Ca^{2+} channels. *Neuron* **12**, 1301–1318 (1994).
16. B. Z. Peterson, C. D. DeMaria, J. P. Adelman, D. T. Yue, Calmodulin is the Ca^{2+} sensor for Ca^{2+}-dependent inactivation of L-type calcium channels. *Neuron* **22**, 549–558 (1999).
17. B. C. Suh, K. Leal, B. Hille, Modulation of high-voltage activated Ca^{2+} channels by membrane phosphatidylinositol 4,5-bisphosphate. *Neuron* **67**, 224–238 (2010).
18. N. Gamper, V. Reznikov, Y. Yamada, J. Yang, M. S. Shapiro, Phosphatidylinositol 4,5-bisphosphate signals underlie receptor-specific $G_{q/11}$-mediated modulation of N-type Ca^{2+} channels. *J. Neurosci.* **24**, 10980–10992 (2004).
19. L. Wu, C. S. Bauer, X. G. Zhen, C. Xie, J. Yang, Dual regulation of voltage-gated calcium channels by PtdIns(4,5)P_2. *Nature* **419**, 947–952 (2002).
20. B. C. Suh, D. I. Kim, B. H. Falkenburger, B. Hille, Membrane-localized beta-subunits alter the PIP_2 regulation of high-voltage activated Ca^{2+} channels. *Proc. Natl. Acad. Sci. U.S.A.* **109**, 3161–3166 (2012).
21. O. Vivas, H. Castro, I. Arenas, D. Elias-Vinas, D. E. Garcia, PIP_2 hydrolysis is responsible for voltage independent inhibition of $Ca_V2.2$ channels in sympathetic neurons. *Biochem. Biophys. Res. Commun.* **432**, 275–280 (2013).
22. L. de la Cruz *et al.*, PIP_2 in pancreatic β-cells regulates voltage-gated calcium channels by a voltage-independent pathway. *Am. J. Physiol. Cell Physiol.* **311**, C630–C640 (2016).
23. E. Kaschina, T. Unger, Angiotensin AT1/AT2 receptors: Regulation, signalling and function. *Blood Press.* **12**, 70–88 (2003).
24. G. W. Dorn II, T. Force, Protein kinase cascades in the regulation of cardiac hypertrophy. *J. Clin. Invest.* **115**, 527–537 (2005).
25. J. G. Burniston, A. Saini, L. B. Tan, D. F. Goldspink, Angiotensin II induces apoptosis in vivo in skeletal, as well as cardiac, muscle of the rat. *Exp. Physiol.* **90**, 755–761 (2005).
26. K. D. Schluter, S. Wenzel, Angiotensin II: A hormone involved in and contributing to pro-hypertrophic cardiac networks and target of anti-hypertrophic cross-talks. *Pharmacol. Ther.* **119**, 311–325 (2008).
27. S. J. Forrester *et al.*, Angiotensin II signal transduction: An update on mechanisms of physiology and pathophysiology. *Physiol. Rev.* **98**, 1627–1738 (2018).
28. O. Ichiyanagi, K. Ishii, M. Endoh, Angiotensin II increases L-type Ca^{2+} current in gramicidin D-perforated adult rabbit ventricular myocytes: Comparison with conventional patch-clamp method. *Pflugers Arch.* **444**, 107–116 (2002).
29. E. A. Aiello, H. E. Cingolani, Angiotensin II stimulates cardiac L-type Ca^{2+} current by a Ca^{2+}- and protein kinase C-dependent mechanism. *Am. J. Physiol. Heart Circ. Physiol.* **280**, H1528–H1536 (2001).
30. I. S. Allen *et al.*, Angiotensin II increases spontaneous contractile frequency and stimulates calcium current in cultured neonatal rat heart myocytes: Insights into the underlying biochemical mechanisms. *Circ. Res.* **62**, 524–534 (1988).
31. T. Hermosilla *et al.*, L-type calcium channel beta subunit modulates angiotensin II responses in cardiomyocytes. *Channels (Austin)* **5**, 280–286 (2011).
32. G. Bkaily *et al.*, Angiotensin II-induced increase of T-type Ca^{2+} current and decrease of L-type Ca^{2+} current in heart cells. *Peptides* **26**, 1410–1417 (2005).
33. W. C. De Mello, Intracellular angiotensin II regulates the inward calcium current in cardiac myocytes. *Hypertension* **32**, 976–982 (1998).
34. P. Varnai, T. Balla, Visualization of phosphoinositides that bind pleckstrin homology domains: Calcium- and agonist-induced dynamic changes and relationship to myo-[3H]inositol-labeled phosphoinositide pools. *J. Cell Biol.* **143**, 501–510 (1998).
35. B. H. Falkenburger, J. B. Jensen, B. Hille, Kinetics of PIP_2 metabolism and KCNQ2/3 channel regulation studied with a voltage-sensitive phosphatase in living cells. *J. Gen. Physiol.* **135**, 99–114 (2010).
36. J. B. Jensen, J. S. Lyssand, C. Hague, B. Hille, Fluorescence changes reveal kinetic steps of muscarinic receptor-mediated modulation of phosphoinositides and Kv7.2/7.3 K^+ channels. *J. Gen. Physiol.* **133**, 347–359 (2009).
37. E. J. Dickson, J. B. Jensen, B. Hille, Golgi and plasma membrane pools of PI(4)P contribute to plasma membrane PI(4,5)P_2 and maintenance of KCNQ2/3 ion channel current. *Proc. Natl. Acad. Sci. U.S.A.* **111**, E2281–E2290 (2014).
38. Z. Gaborik *et al.*, Beta-arrestin- and dynamin-dependent endocytosis of the AT1 angiotensin receptor. *Mol. Pharmacol.* **59**, 239–247 (2001).
39. A. C. Holloway *et al.*, Side-chain substitutions within angiotensin II reveal different requirements for signaling, internalization, and phosphorylation of type 1A angiotensin receptors. *Mol. Pharmacol.* **61**, 768–777 (2002).
40. L. Ferron, S. D. Guderyan, E. J. Smith, G. W. Zamponi, $Ca_V\beta$-subunit dependence of forward and reverse trafficking of $Ca_V1.2$ calcium channels. *Mol. Brain* **15**, 43 (2022).
41. R. Conrad *et al.*, Rapid turnover of the cardiac L-type $Ca_V1.2$ channel by endocytic recycling regulates its cell surface availability. *iScience* **7**, 1–15 (2018).
42. G. Kaur *et al.*, A polybasic plasma membrane binding motif in the I-II linker stabilizes voltage-gated $Ca_V1.2$ calcium channel function. *J. Biol. Chem.* **290**, 21086–21100 (2015).
43. E. P. Cheng *et al.*, Restoration of normal L-type Ca^{2+} channel function during Timothy syndrome by ablation of an anchoring protein. *Circ. Res.* **109**, 255–261 (2011).
44. S. Gao, X. Yao, N. Yan, Structure of human $Ca_V2.2$ channel blocked by the painkiller ziconotide. *Nature* **596**, 143–147 (2021).
45. C. Nasuhoglu *et al.*, Modulation of cardiac PIP_2 by cardioactive hormones and other physiologically relevant interventions. *Am. J. Physiol. Cell Physiol.* **283**, C223–C234 (2002).
46. B. C. Suh, B. Hille, Recovery from muscarinic modulation of M current channels requires phosphatidylinositol 4,5-bisphosphate synthesis. *Neuron* **35**, 507–520 (2002).
47. D. W. Hilgemann, R. Ball, Regulation of cardiac Na^+, Ca^{2+} exchange and $_{KAT}$P potassium channels by PIP_2. *Science* **273**, 956–959 (1996).
48. P. D. Swaminathan, A. Purohit, T. J. Hund, M. E. Anderson, Calmodulin-dependent protein kinase II: Linking heart failure and arrhythmias. *Circ. Res.* **110**, 1661–1677 (2012).
49. S. Kim *et al.*, Angiotensin II induces cardiac phenotypic modulation and remodeling in vivo in rats. *Hypertension* **25**, 1252–1259 (1995).
50. S. D. Crowley *et al.*, Angiotensin II causes hypertension and cardiac hypertrophy through its receptors in the kidney. *Proc. Natl. Acad. Sci. U.S.A.* **103**, 17985–17990 (2006).
51. M. Zhang *et al.*, Contractile function during angiotensin-II activation: Increased Nox2 activity modulates cardiac calcium handling via phospholamban phosphorylation. *J. Am. Coll. Cardiol.* **66**, 261–272 (2015).
52. A. Kameyama, K. Yazawa, M. Kaibara, K. Ozono, M. Kameyama, Run-down of the cardiac Ca^{2+} channel: Characterization and restoration of channel activity by cytoplasmic factors. *Pflugers Arch.* **433**, 547–556 (1997).
53. S. Weiss, S. Oz, A. Benmocha, N. Dascal, Regulation of cardiac L-type Ca^{2+} channel $Ca_V1.2$ via the β-adrenergic-cAMP-protein kinase A pathway: Old dogmas, advances, and new uncertainties. *Circ. Res.* **113**, 617–631 (2013).

54. K. Yamaoka, M. Kameyama, Regulation of L-type Ca^{2+} channels in the heart: Overview of recent advances. *Mol. Cell. Biochem.* **253**, 3–13 (2003).
55. D. W. Hilgemann, Cytoplasmic ATP-dependent regulation of ion transporters and channels: Mechanisms and messengers. *Annu. Rev. Physiol.* **59**, 193–220 (1997).
56. J. B. Seo, S. R. Jung, W. Huang, Q. Zhang, D. S. Koh, Charge shielding of PIP_2 by cations regulates enzyme activity of phospholipase C. *PLoS One* **10**, e0144432 (2015).
57. D. W. Hilgemann, On the physiological roles of PIP_2 at cardiac Na^+ Ca^{2+} exchangers and $_{KAT}$P channels: A long journey from membrane biophysics into cell biology. *J. Physiol.* **582**, 903–909 (2007).
58. B. C. Suh, D. I. Kim, B. H. Falkenburger, B. Hille, Membrane-localized β-subunits alter the PIP_2 regulation of high-voltage activated Ca^{2+} channels. *Proc. Natl. Acad. Sci. U.S.A.* **109**, 3161–3166 (2012), 10.1073/pnas.1121434109.
59. H. M. Colecraft *et al.*, Novel functional properties of Ca(2+) channel β subunits revealed by their expression in adult rat heart cells. *J. Physiol.* **541**, 435–452 (2002).
60. S. X. Takahashi, S. Mittman, H. M. Colecraft, Distinctive modulatory effects of five human auxiliary β_2 subunit splice variants on L-type calcium channel gating. *Biophys. J.* **84**, 3007–3021 (2003).
61. P. Bartels *et al.*, Half-calcified calmodulin promotes basal activity and inactivation of the L-type calcium channel $Ca_V1.2$. *J. Biol. Chem.* **298**, 102701 (2022), 10.1016/j.jbc.2022.102701
62. M. Turner *et al.*, alpha-Actinin-1 promotes activity of the L-type Ca^{2+} channel $Ca_V1.2$. *EMBO J.* **39**, e106171 (2020).
63. O. Vivas, S. A. Tiscione, R. E. Dixon, D. S. Ory, E. J. Dickson, Niemann-pick type C disease reveals a link between lysosomal cholesterol and PtdIns(4,5)P_2 that regulates neuronal excitability. *Cell Rep.* **27**, 2636–2648.e4 (2019).
64. A. Traynor-Kaplan *et al.*, Fatty-acyl chain profiles of cellular phosphoinositides. *Biochim. Biophys. Acta Mol. Cell Biol. Lipids* **1862**, 513–522 (2017).